MD Simulation of Water Using a Rigid Body Description Requires a Small Time Step to Ensure Equipartition

Dilipkumar N. Asthagiri* and Thomas L. Beck*

ACCESS | ⬛ Metrics & More | 📰 Article Recommendations | ⬛ Supporting Information

ABSTRACT: In simulations of aqueous systems, it is common to freeze the bond vibration and angle bending modes in water to allow for a longer time step δt for integrating the equations of motion. Thus, $\delta t = 2$ fs is often used in simulating rigid models of water. We simulate the SPC/E model of water using δt from 0.5 to 3.0 fs and up to 4 fs using hydrogen mass repartitioning. In these simulations, we find that for all but $\delta t = 0.5$ fs, equipartition is not obtained between translational and rotational modes, with the rotational modes exhibiting a lower temperature than the translation modes. To probe the reasons for the lack of equipartition, we study the autocorrelation of the translational velocity of the center of mass and the angular velocity of the rigid water molecule, respectively. We find that the rotational relaxation occurs on a timescale comparable to vibrational periods, calling into question the original motivations for freezing the vibrations. Furthermore, a time step with $\delta t \geq 1$ fs is not able to capture accurately the fast rotational relaxation, which reveals its impact as an effective slowing-down of rotational relaxation. The fluctuation−dissipation relation then leads to the conclusion that the rotational temperature should be cooler for δt greater than the reference value of 0.5 fs. Consideration of fluctuation−dissipation in equilibrium molecular dynamics simulations also emphasizes the need to capture the temporal evolution of fluctuations with fidelity and the role of δt in this regard. The time step also influences the solution thermodynamic properties: both the mean system potential energies and the excess entropy of hydration of a soft repulsive cavity are sensitive to δt.
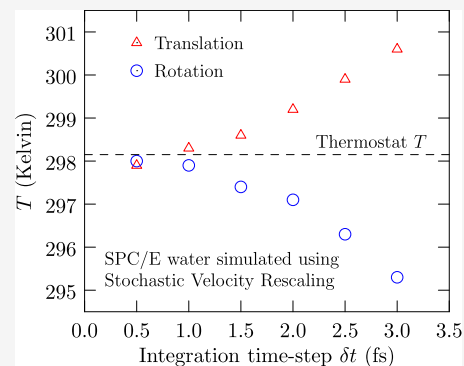

1. INTRODUCTION

Water is the matrix of life, and a molecular-level understanding of biological processes is predicated on understanding how the biomolecules are influenced by the liquid water matrix. Thus, developing better ways to describe the structure and dynamics of water has come to occupy a central position in computational (bio)molecular sciences.

Rahman and Stillinger, the early pioneers in simulating water using molecular dynamics, described water as a rigid object and numerically solved for the coupled translational and rotational motion of each water molecule in the liquid.[1,2] In their numerical scheme, the translational motion of the center of mass was formulated in terms of Cartesian coordinates, and the rotational motion was formulated in terms of Euler angles. The Hamiltonian of the system was based on the sum of Lennard-Jones and electrostatic contributions. Using the mass m of the water molecule, the Lennard-Jones well-depth ε, and the collision diameter σ, they identified the natural unit of time in the equations of motion to be $\tau = \sigma \cdot \sqrt{m/\varepsilon} \approx 2$ ps.[1] From numerical experiments on a two-molecule system, they found that to integrate the coupled set of equations, they had to use a time step $\delta t = 2 \times 10^{-4} \tau \approx 0.4$ fs. They noted that the smallness of this time step, relative to modeling liquid Ar, for example, stemmed from the "rapid angular velocity of the water molecules".[1] We will return to this point below.

A few years after Rahman and Stillinger's work, Ryckaert, Ciccotti, and Berendsen developed the SHAKE algorithm[3] to incorporate holonomic constraints in simulating various types of molecules, including water. For simulating a rigid model of water, one choice of constraints could be the OH bond lengths and the HOH bond angle. These holonomic constraints lead to additional forces in the dynamical equations, but the significant computational advantage that one gains is in formulating all the equations in Cartesian coordinates. Later, Andersen noted that in simulating a rigid object, the relative velocity of atoms connected by a rigid bond should be zero in the direction of the bond. Andersen developed the RATTLE algorithm to include this velocity constraint.[4] More than a decade after Andersen's work, Miyamoto and Kollman[5] presented the SETTLE algorithm specifically for describing water as a rigid molecule. This algorithm obviated the iterations implicit in the SHAKE and RATTLE methods. Like SHAKE, the RATTLE and SETTLE methods require only Cartesian coordinates.
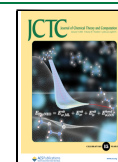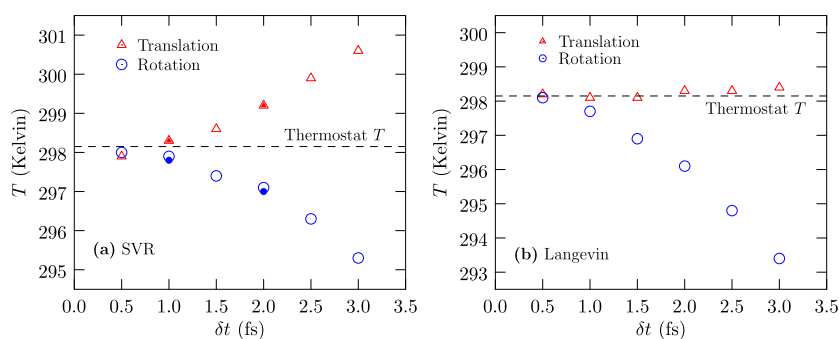
Figure 1. Temperature distribution between the translational and rotational modes in simulations of SPC/E water. The temperatures are based on the mean kinetic energy path. Results using (a) SVR and (b) Langevin thermostats. The open symbols are based on simulations with NAMD.[17,18] The symbol size is about the 2σ standard error of the mean. The filled symbols in (a) are based on simulations using LAMMPS.[19,20]

One of the motivations in developing the SHAKE and subsequent algorithms noted above was to freeze the high-frequency vibrations between bonded pairs of atoms since the "fast internal vibrations are usually decoupled from rotational and translational motions".[3] Since typical vibrational frequencies are about 10^{14} Hz (or a time period of 10 fs), the intuitive idea was that freezing the high-frequency vibrations ought to allow for a longer δt for integrating the equations of motion in molecular simulations. Thus, in the case of simulating rigid water using molecular dynamics, it is very common to use $\delta t = 2$ fs; for example, see refs 6−78. We have used this as well in many of our papers, for example, ref 9. A highly cited paper on protein folding has used $\delta t = 2.5$ fs.[10] Some recent efforts use $\delta t = 4$ fs, albeit by using a larger proton mass and proportionately reducing the oxygen mass, the so-called hydrogen mass repartitioning approach (personal communications, CECAM 2023 meeting on Biomolecular Simulation and Machine Learning in the Exa-Scale Era).

What is the problem, then? In simulation studies on liquid water under supercooled conditions using the Langevin thermostat (Valiya Parambathu and Asthagiri, unpublished), one of us (DNA) noticed that the average temperature from the simulation log was systematically lower than the target by about 1 K. We found the same trend in simulations of hydration of a small amphiphile, *tert*-butanol. This motivated us to examine more thoroughly the distribution of kinetic energy between translational and rotational degrees of freedom in simulations of the rigid SPC/E[11] water model. This examination leads to the finding that for $\delta t \geq 1$ fs, equipartition between translation and rotation is not satisfied, with the problem made worse as δt increases. (We note here that after we had posted a preprint of our work, we became aware of earlier works by Silveira and Abreu[12,13] and Davidchack.[14] These authors had found the same discrepancy between translational and rotational temperatures as here; we shall return to these important studies below.) We examine the physical reason for the breakdown of equipartition and find that $\delta t \geq 1$ limits how well one can capture the fast rotational relaxation. The $\delta t = 0.5$ fs that allows thermalization between rotation and translation is also close to what Rahman and Stillinger[1] used. The violation of equipartition also reveals itself in the δt dependence of the mean potential energy of the system and in the excess entropy of hydration of a soft repulsive cavity, an object of central importance in modeling and analyzing all hydration phenomena.[15,16] As simulations aim for higher fidelity, we recommend that simulations of water, rigid or otherwise, use a time step of 0.5 fs (or less).

2. METHODOLOGY

2.1. Simulation Details. We studied the SPC/E[11] water model using the NAMD[17,18] and LAMMPS[19,20] codes. We studied two system sizes, $N = 2006$ water molecules, which informs the majority of the results, and a limited set of simulations with $N = 16,384$ water molecules noted in the Supporting Information. The volume was adjusted to match the experimental density[21]—33.33 water molecules/nm³ or 0.997 g/cm³—of liquid water at 298.15 K and 1 atm pressure.

For *NVT* simulations, we obtained results using the stochastic velocity rescaling (SVR)[22] and Langevin thermostats, respectively, both of which should correctly sample the canonical distribution. The symplectic velocity-Verlet integrator was used to propagate the dynamics. (Strictly speaking, the symplectic velocity-Verlet integrator is properly called the symplectic momentum Verlet integrator,[23] a point to which we return in the discussion.) For just the first step, the velocities were generated by requiring the velocity of the center of mass of the simulation system to be zero. From *NVT* simulations, we sampled 1050 water molecules (Section S2.2). From the coordinates and velocities of the atoms at a given time point for a sampled water molecule, we calculated the translational kinetic energy of the center of mass and the kinetic energy for rotation about the center of mass. The Supporting Information provides a complete description of the methods (Section S2) and additional supporting results (Section S3).

2.2. Estimating the Temperature. We are interested in the classical statistical mechanics of N water molecules in volume V and temperature T. The physical Hamiltonian of the system comprises separable kinetic and potential energy contributions, with the kinetic energy of each particle being quadratic in the momenta. For simplicity, we consider a single degree of freedom. Then, the probability density distribution of kinetic energies ε_K follows the Maxwell−Boltzmann form

$$f(\varepsilon_K) = \frac{1}{\sqrt{\pi k_B T}} \cdot \frac{1}{\sqrt{\varepsilon_K}} \cdot \exp\left(-\frac{\varepsilon_K}{k_B T}\right) \tag{1}$$

where k_B is the Boltzmann constant and T is the temperature of the thermal bath. $f(\varepsilon_K)$ depends on only one parameter T. For a given set of observations of the kinetic energy, let the mean kinetic energy be $\overline{\varepsilon}_K$. If these observations obey eq 1, we require

$$\frac{k_B T}{2} = \overline{\varepsilon}_K \Rightarrow T = \frac{2\overline{\varepsilon}_K}{k_B} \tag{2}$$

Likewise, the variance $\overline{\delta\varepsilon_K^2} = \overline{\varepsilon_K^2} - \overline{\varepsilon}_K^2$ should obey
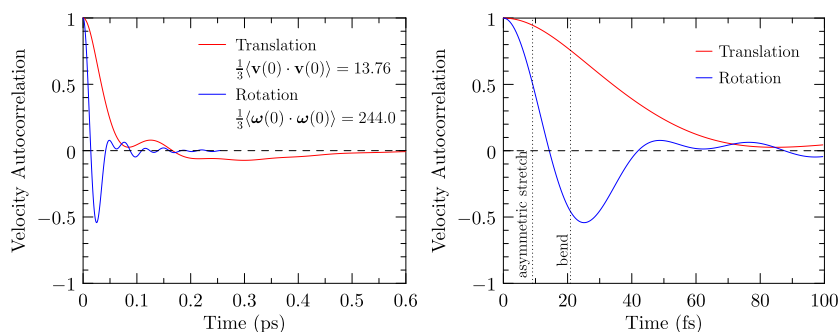
Figure 2. Autocorrelation of the center of mass and angular velocities normalized by the value at time $t = 0$. Time step $\delta t = 0.5$ fs. The average temperature of the simulation cell is 299.6 K with a standard deviation of about 3 K. Left panel: data shown out to 0.6 ps. Right panel: data shown to 100 fs. The time periods associated with the asymmetric stretch and bending modes of a water molecule in the gas phase[26] are also shown for comparison.
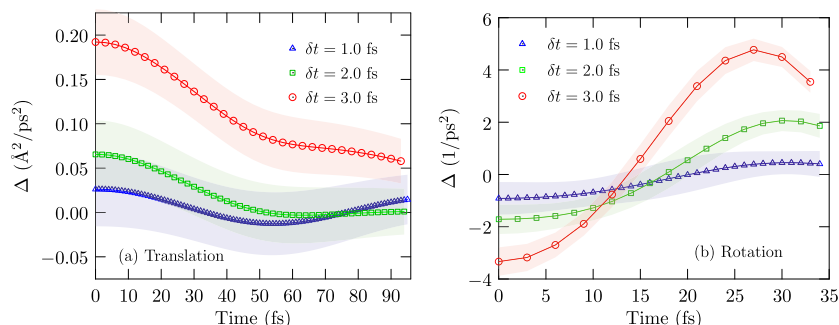

Figure 3. Δ is the difference at a given time point between the autocorrelation for the given δt minus the corresponding reference value by using $\delta t = 0.5$ fs. For no discretization error, $\Delta = 0$. (a) Translational and (b) rotational motion. The shaded area indicates the 1σ standard error of the mean. The mean temperatures of the *NVE* runs are 299.3 K (1.0 fs), 299.1 K (2.0 fs), and 299.7 K (3.0 fs), each with a standard deviation of about 3 K.

$$\overline{\delta\varepsilon_K^2} = \frac{(k_B T)^2}{2} \Rightarrow T = \sqrt{\frac{2}{k_B}}\sqrt{\overline{\delta\varepsilon_K^2}} \tag{3}$$

Thus, given a set of kinetic energies of a particle, we can estimate the parameter T using either the mean value (eq 2) or the variance (eq 3). Note that the variance is but a measure of the heat capacity C_v (of the ideal gas). Consistency between these two estimates, the two moments in eq 1, is a good indicator of adequate sampling.

In comparing observed data of kinetic energies from a simulation versus those from eq 1, one could construct the cumulative distribution from the observed data and infer the T that best describes the cumulative data. In exploratory calculations, we found that comparing T from the two paths noted above works as well as obtaining a T to fit the cumulative distribution function. Thus, for simplicity, we estimate T from eqs 2 and 3.

For a water molecule treated as a rigid body, the total kinetic energy can be partitioned into two contributions: (1) a contribution from the translational motion, $(M/2)\mathbf{v}_{com} \cdot \mathbf{v}_{com}$, where M is the mass of the water molecule and $\mathbf{v}_{com}$ is the center-of-mass velocity; and (2) a contribution from rotation about the center of mass, $0.5\mathbf{w}' \cdot \overline{\overline{I}} \cdot \mathbf{w}$, where $\overline{\overline{I}}$ is the moment of inertia tensor and the $\mathbf{w}$ is the angular velocity, with a transpose indicated by a prime. As discussed in the Supporting Information (Section S1), we calculate $\mathbf{w}$ from site velocities that are readily accessible from simulations[24] (see also ref 25).

3. RESULTS AND DISCUSSION

Figure 1 shows that the temperatures ascribable to the different modes converge only for $\delta t = 0.5$ fs (see also refs 12−14).

For the Langevin thermostat with $\delta t = 2.0$ fs, the mean of the translational and rotational temperatures is about 297 K, a Kelvin lower than the set point, consistent with the earlier observations for supercooled water and the hydration of the amphiphile that motivated the present work. Similar deviations persist in constant energy (*NVE*) simulations as well (Section S3.4), emphasizing that the data in Figure 1 is not an artifact of the thermostat.

To better understand the results shown in Figure 1, it proves helpful to examine the velocity autocorrelation function. To this end, we take the last configuration of the $\delta t = 0.5$ fs run with the SVR thermostat and launch constant energy runs for 20 ps, saving velocities and positions every time step. For *NVE* starting velocities, we use the same seed for the random number generator for the different δt cases. (For the $\delta t = 2$ or 3 fs cases, it became necessary to start at a slightly higher temperature of 300 K to ensure the mean temperature of the simulation settles close to the value obtained using $\delta t = 0.5$ fs.)

Figure 2 shows the velocity autocorrelation using the data from the $\delta t = 0.5$ fs simulations as our reference. In passing, we note that the integral of the velocity autocorrelation gives the diffusion coefficient through the Green−Kubo relations. As a check, for $\delta t = 0.5$ fs, we find the translational diffusion coefficient using both the Green−Kubo approach and the Einstein relation (Section S3.6) for the mean squared displacement. These estimates agree within the statistical uncertainties.

What is striking about Figure 2 (left panel) is that the rotational motion relaxes considerably faster than the translational motion—observe that the initial value is much higher and thus the decay much faster for the autocorrelation of the angular velocity. This is consistent with what Rahman and Stillinger[1]

noted. Physically, the rotational relaxation is considerably faster than the translational relaxation because the small mass of the proton relative to that of the oxygen means that the moment of inertia (about the axes through the center of mass) is small, and rotations are sensitive to small torques. In contrast, the translation motion would be considerably less sensitive to small forces because the forces operate on the total mass of the water molecule.

As Figure 2 (right panel) shows, the rotational relaxation occurs over timescales that are similar to the time period of the bond vibration and angle bending modes of a water molecule in the gas phase. For a water molecule in the liquid, because of hydrogen bonding interactions, these modes will be softened, i.e., red-shifted, and spread out.[26] Therefore, even using the worst-case estimate of a water molecule in the gas phase, we find that the original motivation for freezing vibrations is not well-founded for describing liquid water. This is a distinguishing and significant conclusion of the present work.

Figure 3 shows the difference between the velocity autocorrelation functions obtained using a given δt and the reference values based on $\delta t = 0.5$ fs (Figure 2). We focus on the initial times, as this is the most important and sensitive part of the overall relaxation. It is immediately clear that the discretization of the equations of motion limits the fidelity with which we can assess the corresponding relaxation. For the translational motion (Figure 3, left panel), the differences at initial times are all positive. However, the net impact on the diffusion coefficient as assessed by the Einstein relation is small (Section S3.6); this suggests that integrating the overall autocorrelation can smooth out errors and mask the role of δt. Similarly, for the rotational motion (Figure 3, right panel), we find that the autocorrelation up to about 15 fs is lower than the reference value. Notice the stark contrast in the magnitudes of the deviations relative to the reference autocorrelation. Since rotational relaxation occurs on a considerably shorter timescale and involves larger magnitudes, it is also more sensitive to discretization: large δt leads to larger errors in describing rotational relaxation than it does for translational relaxation.

We can use the fluctuation−dissipation relation $\mathcal{D} = k_{\mathrm{B}}T/\xi$, where $\mathcal{D}$ is the diffusion coefficient (and a measure of fluctuations), ξ is the friction (and a measure of dissipation), and $k_{\mathrm{B}}T$ is the thermal energy, to interpret the results above. Treating $\xi/k_{\mathrm{B}}T$ as "effective" friction, and focusing on the initial time behavior of the autocorrelation, we can infer that the "effective" friction appears to be higher for rotational motion and lower for translational motion relative to the $\delta t = 0.5$ fs reference. Friction arises due to intermolecular interactions. Since the same potential model is used for all δt values, a high "effective" friction is a consequence of lower temperature and vice versa, in agreement with the results in Figure 1.

Computing the frequency spectrum of the velocity autocorrelation is also instructive in highlighting the limitations the choice of δt imposes on our ability to resolve temporal phenomena. Imagine sampling a temporal signal at δt intervals. The Nyquist−Shannon sampling theorem[27−29] then says that the critical upper frequency that can be correctly captured is $1/(2\delta t)$; trying to capture higher frequencies will necessarily involve aliasing, i.e., spurious low-frequency artifacts get folded into the Fourier spectrum. In the context of molecular dynamics simulations, the sampling theorem leads to the conclusion that for a time step of δt, we are limited to describing phenomena with time periods $\geq 2\delta t$. As Figure 2 (right panel) shows and is readily confirmed by the frequency spectrum in Figure 4, over

this timescale there is considerable variability in the relaxation (for $t \leq 6$ fs), whose effect can never be well captured.
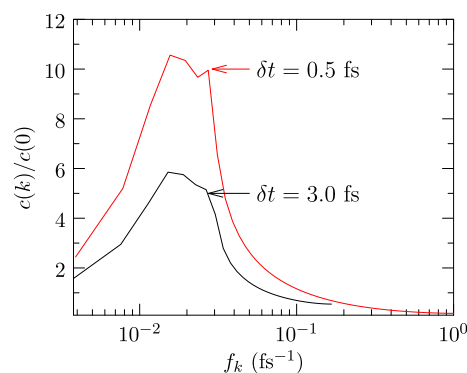

Figure 4. Frequency spectrum of the angular velocity autocorrelation for different time steps. $c(k)$ is the absolute magnitude of the Fourier coefficient; f_k is the frequency of the kth Fourier mode. Specifically, $f_k = k/(\delta t \cdot N)$, where $N + 1$ is the total number of data points in the input signal, including time $t = 0$. δt is the time step and also the time interval at which the data was stored. Note that the curves are cutoff at the Nyquist frequency.

The fluctuation−dissipation theorem then assures us that this limitation will impact our estimate of the temperature.

We hypothesized that the discrepancy in thermalization between rotational and translational motions ought to influence properties besides initial relaxation, including thermodynamic properties such as excess entropy. To test this hypothesis, we first calculated the mean binding energy, $\langle\varepsilon\rangle$, of a water molecule with the rest of the system (Section S2.1.4)—the mean potential energy of the N water molecule system is $N\langle\varepsilon\rangle/2$. Figure 5 (left panel) shows that the mean binding energy is indeed sensitive to δt, with the values obtained using different thermostats converging only for $\delta t = 0.5$ fs. Specifically, for $\delta t = 3$ fs, the mean potential energy per water molecule differs by 0.3% between the two thermostats; for $\delta t = 0.5$ fs, the deviation drops to 0.03%. This result suggests that the water reorganization enthalpies will be sensitive to δt.

Figure 5 (right panel) shows the hydration-free energy of a soft repulsive cavity of size 4 Å (Section S2.3) as a function of temperature. The excess entropy of hydration at 298.15 K obtained from a linear fit to the μ^{ex} data is -12.8 ± 0.1 cal/(mol K) for $\delta t = 0.5$ fs and -18.6 ± 0.1 cal/(mol K) for $\delta t = 2.0$ fs, a nearly 50% difference. The free energies themselves are about the same at 298.15 K, suggesting a compensation between enthalpic and entropic effects.

The identification of fast rotational relaxation of water by us is certainly not new. For example, an early pioneering study by Lawrence and Skinner[30] (see their Figure 4) conveys this point, as does Figure 2 in this work. It is encouraging, and also humbling, that Rahman and Stillinger[1] chose a small δt to better describe the fast angular relaxation, especially at a time when simulations were a lot more demanding than they are now. The key finding of our work is that not capturing the fast rotational relaxation of water can alter the expected equipartition itself.

Earlier researchers[23,31,32] have shown that in discrete Hamiltonian dynamics, the evolution of the system follows a so-called shadow Hamiltonian, which is a function of δt (Section S3.3). This confounds the relationship between momentum (which is what one calculates using the "velocity"-Verlet equations) and velocity in classical mechanics.[23] Thus, it has
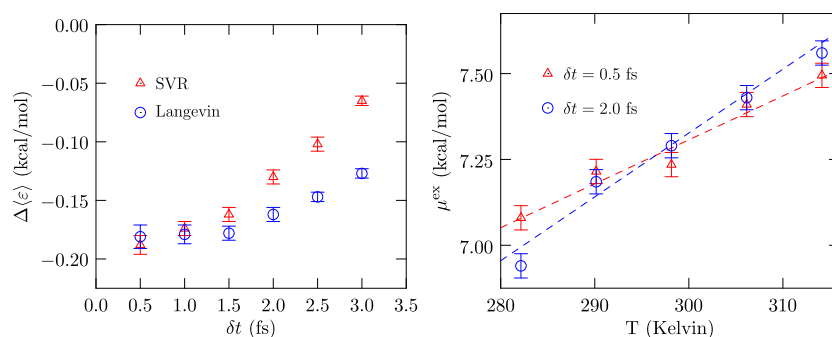
Figure 5. Left panel: mean binding (interaction) energy of a water molecule with the rest of the system: $\Delta\langle\varepsilon\rangle = \langle\varepsilon\rangle - 22$. The standard error of the mean value is at the 2σ level. Note that a deviation of 0.1 kcal/mol per particle amounts to $\approx$200 kcal/mol for the entire system. Right panel: δt dependence of the hydration-free energy of a soft repulsive cavity. The standard error of the mean is shown at the 1σ level.

been argued that the velocity-Verlet velocities are not the most appropriate quantities for estimating the temperature.[23,32] However, the on-step velocity-Verlet velocities are the quantities used in most codes for calculating the instantaneous temperature.

As noted in the Introduction, after we had posted a preprint of the present study, we became aware of careful investigations by Silveira and Abreu[12,13] and Davidchack[14] that have a bearing on this work. Both groups had already noted the kind of discrepancy we find in Figure 1. Tying with the points noted in the preceding paragraph, Davidchack makes the important point that part of the reason for the artifacts to emerge is simply that we measure the properties of the original system while simulating a shadow Hamiltonian. Nevertheless, the breakdown of equipartition in the physical system is a problem, with tangible thermodynamic consequences (for example, Figure 5). To overcome the time-step artifacts, Davidchack suggests combining thermodynamic data from different time-step-based simulations and using Richardson's extrapolation, or using a weighted thermostat. Silveira and Abreu[12] develop an updated formulation to describe the translation and rotation that can avoid energy drifts up to 5 fs time steps. However, as their work makes clear, removing a drift in total energy is not enough to guarantee that equipartition is satisfied. In a subsequent study,[13] Silveira and Abreu have also presented a refined version of kinetic and potential energies that can serve as a better estimator of the shadow Hamiltonian (also see ref 32 in this regard). Our work here confirms the central observations of the breakdown of equipartition noted in these earlier studies. Importantly, whether one uses a refined estimator for the shadow Hamiltonian or not, not capturing the fast rotational relaxation adequately will always be a problem for simulations using a large time step.

One possible way to temper the discretization error and use a larger time step in modeling equilibrium properties is to redistribute the mass between hydrogen and oxygen in a water molecule. In this so-called hydrogen mass repartitioning approach, the mass of hydrogen is increased (usually to 3 amu), and the mass of oxygen is reduced by twice that amount. While this repartitioning scheme will temper the sensitivity of rotations to small torques, we find (Section S3.5) that the repartitioning scheme will still lead to breakdown of equipartition for the time step of 4 fs often used in this approach.

4. CONCLUSIONS

The assumption that fast internal vibrations are decoupled from translational and rotational motions gave birth to a coarse-grained description of water wherein bond vibrations and angle

bending modes are frozen, and a long time step is used to integrate the equations of motion. We find that for water, the rotational relaxation occurs at timescales comparable to bond vibration and angle bending modes. Thus, the original motivation for freezing the vibrational modes is not well-founded for describing water.

In a dynamical simulation at equilibrium, the temporal character of molecular fluctuations, the coefficient of the corresponding dissipative process, and the temperature are intertwined. This implies that it is essential to capture the temporal character of the relaxation process with fidelity. Furthermore, the Nyquist−Shannon sampling theorem emphasizes that for a sampling interval of δt, we can only resolve the temporal phenomena of time period $\geq 2\delta t$. For water described as a rigid body, the autocorrelation of the angular velocity about the center of mass relaxes considerably faster than the autocorrelation of the center-of-mass translational velocity. Since it is essential to capture both relaxation effects correctly to ensure equipartition, the fast relaxation of the angular velocity autocorrelation imposes the upper limit on the time step that is satisfactory. We find here that $\delta t \leq 0.5$ fs is needed to accurately model the molecular dynamics of water using a rigid body description.

The time-step effects are seen in thermodynamic quantities, notably the potential energy per particle and in the entropy of hydration of a soft repulsive cavity. The latter suggests that rate processes are likely to be sensitive to time-step artifacts as well. We leave it to future studies to examine this and to revisit earlier significant results in aqueous phase chemistry and biology that are based on molecular simulations using a large time step. Our findings may also prove relevant to efforts in coarse-graining simulations and in the development and benchmarking of force fields.

■ ASSOCIATED CONTENT

Ⓢ Supporting Information

The Supporting Information is available free of charge at https://pubs.acs.org/doi/10.1021/acs.jctc.3c01153.

> Simulation systems, codes, time steps, calculation of translational and rotational kinetic energy, calculation of the hydration-free energy of a soft repulsive cavity, tabulated data for results in Figure 1, data for relative velocity along constrained bonds, sampling of the shadow Hamiltonian, translational and rotational energy in *NVE* simulations using either a constraint algorithm or rigid body dynamics, influence of the proton mass for $\delta t = 4$ fs,

and mean squared displacement for translational diffusion coefficient (PDF)

■ AUTHOR INFORMATION

Corresponding Authors

Dilipkumar N. Asthagiri − *Oak Ridge National Laboratory, Oak Ridge, Tennessee 37830-6012, United States;* ◉ orcid.org/0000-0001-5869-0807; Email: asthagiridn@ornl.gov

Thomas L. Beck − *Oak Ridge National Laboratory, Oak Ridge, Tennessee 37830-6012, United States;* ◉ orcid.org/0000-0001-8973-7145; Email: becktl@ornl.gov

Complete contact information is available at:
https://pubs.acs.org/10.1021/acs.jctc.3c01153

Notes

The authors declare no competing financial interest.

■ ACKNOWLEDGMENTS

■ REFERENCES

(1) Rahman, A.; Stillinger, F. H. Molecular Dynamics Study of Liquid Water. *J. Chem. Phys.* **1971**, *55*, 3336−3359.

(2) Stillinger, F. H.; Rahman, A. Improved Simulation of Liquid Water by Molecular Dynamics. *J. Chem. Phys.* **1974**, *60*, 1545−1557.

(3) Ryckaert, J. P.; Ciccotti, G.; Berendsen, H. J. C. Numerical Integration of the Cartesian Equations of Motion of a System with Constraints: Molecular Dynamics of n-alkanes. *J. Comput. Phys.* **1977**, *23*, 327−341.

(4) Andersen, H. C. Rattle: A Velocity Version of the Shake Algorithm for Molecular Dynamics Calculations. *J. Comput. Phys.* **1983**, *52*, 24−34.

(5) Miyamoto, S.; Kollman, P. A. Settle: An Analytical Version of the SHAKE and RATTLE Algorithm for Rigid Water Models. *J. Comput. Chem.* **1992**, *13*, 952−962.

(6) Hummer, G.; Rasaiah, J. C.; Noworyta, J. P. Water Conduction Through the Hydrophobic Channel of a Carbon Nanotube. *Nature* **2001**, *414*, 188−190.

(7) Paschek, D. Temperature Dependence of the Hydrophobic Hydration and Interaction of Simple Solutes: An Examination of Five Popular Water Models. *J. Chem. Phys.* **2004**, *120*, 6674−6690.

(8) Godawat, R.; Jamadagni, S. N.; Garde, S. Characterizing Hydrophobicity of Interfaces by using Cavity Formation, Solute Binding, and Water Correlations. *Proc. Natl. Acad. Sci. U.S.A.* **2009**, *106*, 15119−15124.

(9) Tomar, D. S.; Paulaitis, M. E.; Pratt, L. R.; Asthagiri, D. N. Hydrophilic Interactions Dominate the Inverse Temperature Dependence of Polypeptide Hydration Free Energies Attributed to Hydrophobicity. *J. Phys. Chem. Lett.* **2020**, *11*, 9965−9970.

(10) Lindorff-Larsen, K.; Piana, S.; Dror, R. O.; Shaw, D. E. How Fast-Folding Proteins Fold. *Science* **2011**, *334*, 517−520.

(11) Berendsen, H. J. C.; Grigera, J. R.; Straatsma, T. P. The Missing Term in Effective Pair Potentials. *J. Phys. Chem.* **1987**, *91*, 6269−6271.

(12) Silveira, A. J.; Abreu, C. R. A. Molecular Dynamics with Rigid Bodies: Alternative Formulation and Assessment of its Limitations when Employed to Simulate Liquid Water. *J. Chem. Phys.* **2017**, *147*, 124104.

(13) Silveira, A. J.; Abreu, C. R. A. Refinement of Thermostated Molecular Dynamics using Backward Error Analysis. *J. Chem. Phys.* **2019**, *150*, 114110.

(14) Davidchack, R. L. Discretization Errors in Molecular Dynamics Simulations with Deterministic and Stochastic Thermostats. *J. Comput. Phys.* **2010**, *229*, 9323−9346.

(15) Pratt, L. R.; Pohorille, A. Theory of Hydrophobicity: Transient Cavities in Molecular Liquids. *Proc. Natl. Acad. Sci. U.S.A.* **1992**, *89*, 2995−2999.

(16) Pratt, L. R. Molecular Theory of Hydrophobic Effects: "She Is Too Mean To Have Her Name Repeated. *Annu. Rev. Phys. Chem.* **2002**, *53*, 409−436.

(17) Kale, L.; Skeel, R.; Bhandarkar, M.; Brunner, R.; Gursoy, A.; Krawetz, N.; Phillips, J.; Shinozaki, A.; Varadarajan, K.; Schulten, K. NAMD2: Greater Scalability for Parallel Molecular Dynamics. *J. Comput. Phys.* **1999**, *151*, 283−312.

(18) Phillips, J. C.; Hardy, D. J.; Maia, J. D. C.; Stone, J. E.; Ribeiro, J. V.; Bernardi, R. C.; Buch, R.; Fiorin, G.; Hénin, J.; Jiang, W.; et al. Scalable Molecular Dynamics on CPU and GPU Architectures with NAMD. *J. Chem. Phys.* **2020**, *153*, 044130.

(19) Plimpton, S. Fast Parallel Algorithms for Short-Range Molecular Dynamics. *J. Comput. Phys.* **1995**, *117*, 1−19.

(20) Thompson, A. P.; Aktulga, H. M.; Berger, R.; Bolintineanu, D. S.; Brown, W. M.; Crozier, P. S.; in't Veld, P. J.; Kohlmeyer, A.; Moore, S. G.; Nguyen, T. D.; et al. LAMMPS - A Flexible Simulation Tool for Particle-Based Materials Modeling at the Atomic, Meso, and Continuum Scales. *Comput. Phys. Commun.* **2022**, *271*, 108171.

(21) Lemmon, E. W.; McLinden, M. O.; Friend, D. G. Chapter Thermophysical Properties of Fluid Systems. *NIST Chemistry WebBook, NIST Standard Reference Database Number 69*; Linstrom, P. J., Mallard, W. G., Eds.; National Institute of Standards and Technology: Gaithersburg, MD, 2016. http://webbook.nist.gov (retrieved December 2016).

(22) Bussi, G.; Donadio, D.; Parrinello, M. Canonical Sampling Through Velocity Rescaling. *J. Chem. Phys.* **2007**, *126*, 014101.

(23) Gans, J.; Shalloway, D. Shadow Mass and the Relationship Between Velocity and Momentum in Symplectic Numerical Integration. *Phys. Rev. E: Stat. Phys., Plasmas, Fluids, Relat. Interdiscip. Top.* **2000**, *61*, 4587−4592.

(24) Singer, P. M.; Asthagiri, D.; Chapman, W. G.; Hirasaki, G. J. NMR Spin-Rotation Relaxation and Diffusion of Methane. *J. Chem. Phys.* **2018**, *148*, 204504.

(25) Palmer, J. C.; Haji-Akbari, A.; Singh, R. S.; Martelli, F.; Car, R.; Panagiotopoulos, A. Z.; Debenedetti, P. G. Comment on "The putative liquid-liquid transition is a liquid-solid transition in atomistic models of water" [I and II: J. Chem. Phys. 135, 134503 (2011); J. Chem. Phys. 138, 214504 (2013)]. *J. Chem. Phys.* **2018**, *148*, 137101.

(26) Kananenka, A. A.; Skinner, J. L. Fermi Resonance in OH-stretch Vibrational Spectroscopy of Liquid Water and the Water Hexamer. *J. Chem. Phys.* **2018**, *148*, 244107.

(27) Shannon, C. Communication in the Presence of Noise. *Proc. IRE* **1949**, *37*, 10−21.

(28) Nyquist, H. Certain Topics in Telegraph Transmission Theory. *Trans. Am. Inst. Electr. Eng.* **1928**, *47*, 617−644.

(29) Press, W. H.; Teukolsky, S. A.; Vellerling, W. T.; Flannery, B. P. Chapter 12 Fast Fourier Transforms. *Numerical Recipes in Fortran*, 2nd ed.; Cambridge University Press, 1992.

(30) Lawrence, C. P.; Skinner, J. L. Vibrational Spectroscopy of HOD in liquid D_2O. I. Vibrational Energy Relaxation. *J. Chem. Phys.* **2002**, *117*, 5827−5838.

(31) Toxvaerd, S. Hamiltonians for discrete dynamics. *Phys. Rev. E: Stat. Phys., Plasmas, Fluids, Relat. Interdiscip. Top.* **1994**, *50*, 2271−2274.

(32) Eastwood, M. P.; Stafford, K. A.; Lippert, R. A.; Jensen, M. Ø.; Maragakis, P.; Predescu, C.; Dror, R. O.; Shaw, D. E. Equipartition and the Calculation of Temperature in Biomolecular Simulations. *J. Chem. Theory Comput.* **2010**, *6*, 2045−2058.